Supporting Information for

Self-Assembly of Amphiphilic Asymmetric Comb-Like Copolymers with Responsive Rigid Side Chains

Zhengyi Li,‡ Weisheng Feng,‡ Xing Zhang, Binbin Xu,* Liquan Wang, Shaoliang Lin*

Shanghai Key Laboratory of Advanced Polymeric Materials, Key Laboratory for Ultrafine Materials of Ministry of Education, Frontiers Science Center for Materiobiology and Dynamic Chemistry, School of Materials Science and Engineering, East China University of Science and Technology, Shanghai 200237, China

*E-mail: binbinxu@ecust.edu.cn; slin@ecust.edu.cn

1. Simulation Method

The DPD method is a coarse-grained, mesoscopic simulation technique, which was first introduced by Hoogerbrugge and Koelman[1] in 1992 and improved by Español and Warren[2,3] in 1995. In DPD method, one coarse-grained bead represents a group of atoms, DPD beads obey Newton's equation of motion (1), and the forces acting on DPD beads include three parts: conservative force ($\mathbf{F}_{ij}^{\mathrm{C}}$), dissipative force ($\mathbf{F}_{ij}^{\mathrm{D}}$), and random force ($\mathbf{F}_{ij}^{\mathrm{R}}$).

$$\frac{\mathrm{d}\mathbf{r}_i}{\mathrm{d}t} = \mathbf{v}_i, \; m_i \frac{\mathrm{d}\mathbf{v}_i}{\mathrm{d}t} = \mathbf{f}_i \tag{S1}$$

$$\mathbf{f}_i = \sum_{i \neq j} (\mathbf{F}_{ij}^{\mathrm{C}} + \mathbf{F}_{ij}^{\mathrm{D}} + \mathbf{F}_{ij}^{\mathrm{R}}) \tag{S2}$$

$$\mathbf{F}_{ij}^{\mathrm{C}} = \omega^{\mathrm{C}}(r_{ij})\hat{\mathbf{r}}_{ij} \tag{S3}$$

$$\mathbf{F}_{ij}^{\mathrm{D}} = -\gamma\omega^{\mathrm{D}}(r_{ij})(\hat{\mathbf{r}}_{ij} \cdot \mathbf{v}_{ij})\hat{\mathbf{r}}_{ij} \tag{S4}$$

$$\mathbf{F}_{ij}^{\mathrm{R}} = \sigma\omega^{\mathrm{R}}(r_{ij})\zeta_{ij}\hat{\mathbf{r}}_{ij} \tag{S5}$$

where, the DPD beads are marked by i = 1, 2, ……, N, m_i is the mass of particle i, $\mathbf{f}_i$ is the total force on particle i. $\mathbf{r}_{ij} = \mathbf{r}_i - \mathbf{r}_j$ is the position vector between DPD beads. $r_{ij} = |\mathbf{r}_{ij}|$, $\hat{\mathbf{r}}_{ij} = \mathbf{r}_{ij} / r_{ij}$, $\mathbf{v}_{ij} = \mathbf{v}_i - \mathbf{v}_j$ is the velocity difference between DPD beads. γ and σ are the friction and noise strength, respectively. The term ζ_{ij} is Gaussian white noise which is symmetric $\zeta_{ij} = \zeta_{ji}$ and satisfies the properties. ω^{C}, ω^{D}, and ω^{R} are weight functions that describe the range of the conservative, dissipative, and random forces.

$$\omega^{\mathrm{C}}(r_{ij}) = \begin{cases} a_{ij}(1 - r_{ij} / r_{\mathrm{c}}) & r_{ij} \leq r_{\mathrm{c}} \\ 0 & r_{ij} > r_{\mathrm{c}} \end{cases} \tag{S6}$$

$$\omega^{\mathrm{D}}(r_{ij}) = [(\omega^{\mathrm{R}}(r_{ij}))]^2 = \omega(r_{ij}) = \begin{cases} 2(1 - r_{ij} / r_{\mathrm{c}}) & r_{ij} \leq r_{\mathrm{c}} \\ 0 & r_{ij} > r_{\mathrm{c}} \end{cases} \tag{S7}$$

where r_{c} is the range of DPD interactions (cutoff radius). a_{ij} is the interaction parameter between the particles i and j.

It is worth noting that the mass, length, time and energy in DPD all use reduced units, expressed by m, r_c, τ and $k_B T$ respectively, where $m = r_c = k_B T = 1.0$ and $\tau = r_c\sqrt{m/k_B T}$.

In order to construct the coarse-grained model of AACCs, the Bead-Spring model is introduced to apply an additional spring potential connection between two adjacent beads, the expression of which is as follows

$$\mathbf{F}_{ij}^{S} = C(1 - r_{ij} / r_{eq})\hat{\mathbf{r}}_{ij} \tag{S8}$$

where C is the spring constant and r_{eq} denotes the equilibrium bond length. We have chosen C = 100, $r_{eq} = 0.86\, r_c$.

The angle force F^A is given by

$$\mathbf{F}^{A} = -\nabla_{\theta}\left[k_A (\theta - \pi)^2 \right] \tag{S9}$$

where k_A is the angle constant and θ is the bond angle. In this work, k_A was set to 80 to ensure the rigidity of rod blocks.

2. Five independent simulation results of channelized micelles

Fig. S1 shows five independent simulation results of A_{15}-*g*-(C_3/A-$3R_4$), z = 1. The copolymer molecules may aggregate into one channelized micelles (Figure S1a) or one channelized micelles with small vesicles (Figure S1c). The situation greatly depends on the polymer concentration and the box size. The results for five morphologies are similar, which means that the results of the five replicate simulations end up in the same phase.

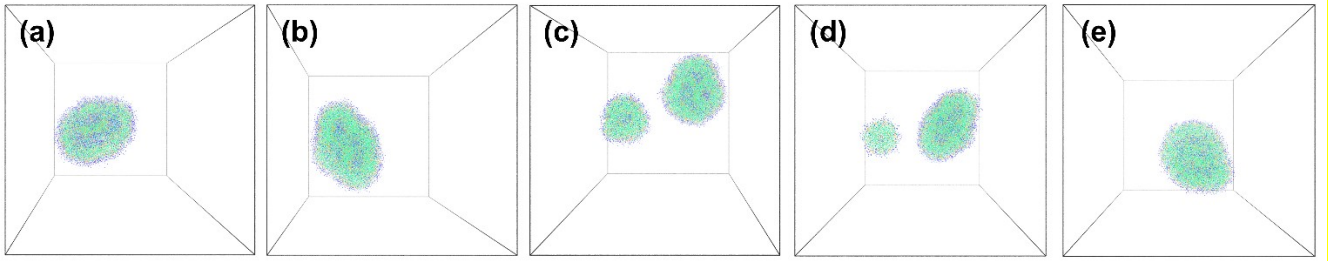

Fig. S1 Five independent simulation results of A_{15}-*g*-(C_3/A-$3R_4$), z = 1, where the polymer concentration is 5%.

3. One-dimensional density profiles of A and C blocks along X arrow for other various aggregates

Except for the channelized micelles, the one-dimensional density profiles of **A**, **C** and **R** segments for other aggregates were calculated to clearly demonstrate their internal structures. As shown in Fig. S2a, in the case of multicompartmental vesicles, **C** blocks exhibit multiple small peaks, corresponding to several solvophilic cavities within the aggregates. Both tube vesicles and spherical vesicles display similar density distributions; specifically, the **A** and **C** blocks have four peaks, while the B blocks have two peaks (Fig. S2b,c). In contrast, for disk-like micelles (Fig. S2d), solvophilic cavities are absent within the aggregates, resulting in the appearance of only two solvophilic peaks and one solvophobic peak.

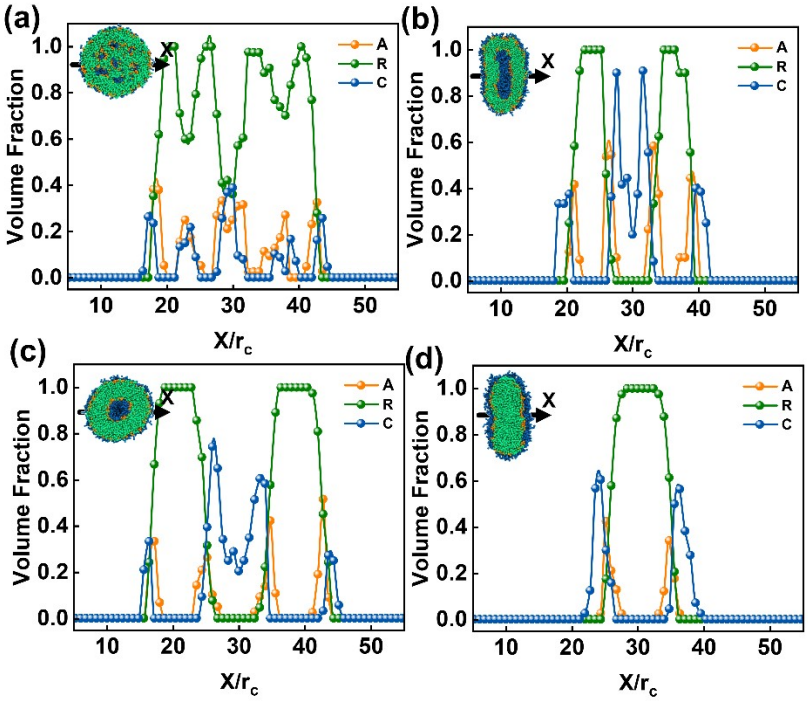

Fig. S2 One-dimensional density profiles of **A** and **C** blocks along X arrow for various aggregates: (a) multicompartmental vesicles, $\mathbf{A}_{15}$-*g*-($\mathbf{C}_2$/$\mathbf{A}_1$-3$\mathbf{R}_5$), z = 1; (b) tube vesicles, **$\mathbf{A}_{15}$-*g*-($\mathbf{C}_5$/$\mathbf{A}_1$-3$\mathbf{R}_5$)**, z = 1; (c) spherical vesicles, $\mathbf{A}_{15}$-*g*-($\mathbf{C}_6$/$\mathbf{A}_1$-3$\mathbf{R}_5$), z = 1; (d) disk-like micelles, $\mathbf{A}_{15}$-*g*-($\mathbf{C}_6$/$\mathbf{A}_1$-3$\mathbf{R}_8$), z = 1.

4. Orientational Arrangement of Rod Pedants

We used the order parameter S to evaluate the orientational arrangement of rod blocks in self-assembled aggregates. The order parameter S is defined as[4,5]

$$S = \frac{\sum_{i=1}^{N_P} \sum_{j=1}^{N_i^*} \left(\frac{3\cos^2 \theta_{ij} - 1}{2} \right)}{\sum_{i=1}^{N_P} N_i^*} \tag{S9}$$

where θ represents the angle between two rigid chains, N_P represents the total number of rigid chains in the aggregates, N_i^* represents the total number of rigid chains adjacent to the ith rigid chain. N_i^* can be determined by calculating the total number of rigid chains in the cylindrical region centered on chain segment i. Any rigid chain with one or more beads within the cylindrical region is considered to be adjacent, and the radius of the cylindrical region is the radius of gyration R_g of the chain segment and the length is the end distance R_e of chain segment i. For rigid chains

$$R_g \approx (1/2\sqrt{3})R_e \tag{S10}$$

However, when the rigid chain segments are short, the local order parameter rises abnormally, we fixed the values of R and L to be 2.0 r_c and 4.0 r_c. From the above, it can be seen that a value of 1 for S indicates that the adjacent rigid chains are completely parallel; a value of 0 for S indicates that the rigid chains are in a completely disordered state.

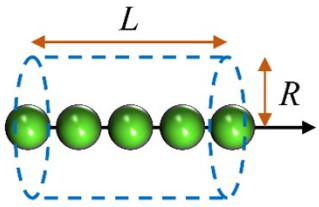

Fig. S3 Schematic diagram of a rigid chain cylinder area when calculating short-range order parameter, where L and R denote the length and radius of the cylinder, respectively.

5. Arrangements of AACCs chains in different aggregates

Fig.S4 shows the arrangements of AACCs chains in different aggregates. As shown, each AACC chains aggregate with itself rather than stretches in aggregates. The arrangement of rigid chains is not uniform, even though they are in the same copolymer chain, which indicates that the self-assembly behaviours of AACCs are mainly affected by the AACC structure and the phase separation between different blocks rather than the orientational arrangement of rigid chains.

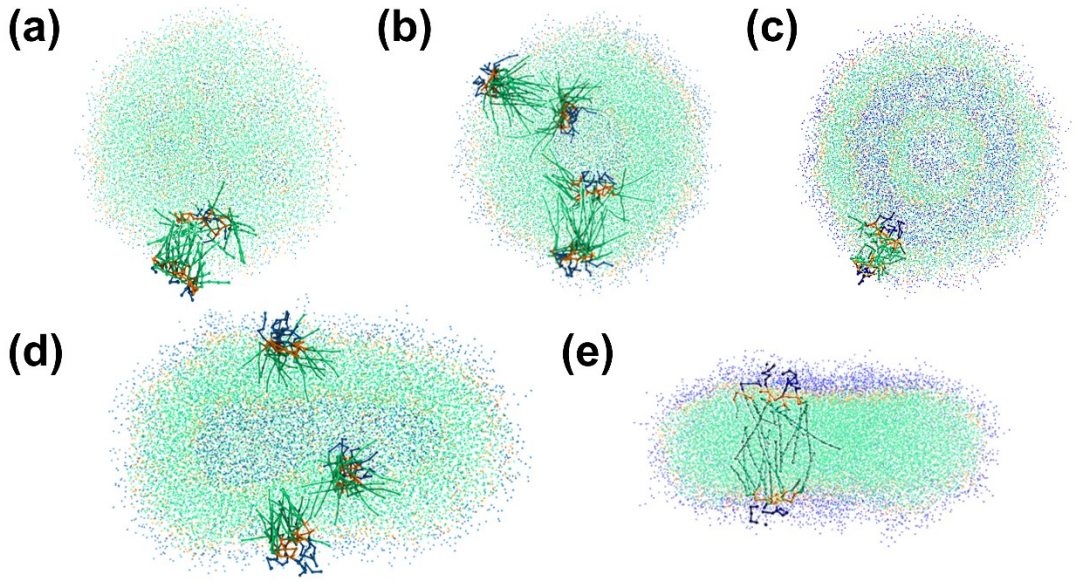

Fig. S4 Arrangements of AACCs chains in (a) multicompartment vesicles (**MV**), (b) spherical vesicles (**SV**), (c) channelized micelles (**CM**), (d) tube vesicles (**TV**), and (e) disk-like micelles (**DM**).

6. Local order parameter of the rigid chains with different spacer numbers

Figure S5 illustrates local order parameter of the rigid chains within the aggregates formed by A_{15}-*g*-(C_4/A-*m*R_3) with different spacer numbers *z* and rigid chain branches *m*. As shown, the local order parameter gradually increases with the increase of the spacer numbers. The increase of the spacer numbers leads to the enhancement of the flexibility of the main chain, which is favourable to the movement of the rigid chain segments and easier to form an ordered structure. When the number of spacer z is certain, with the increase of the branch numbers, the steric effect between the rigid chains increases, which hinders the orderly arrangement of the rigid chains, so the local order parameter decreases gradually.

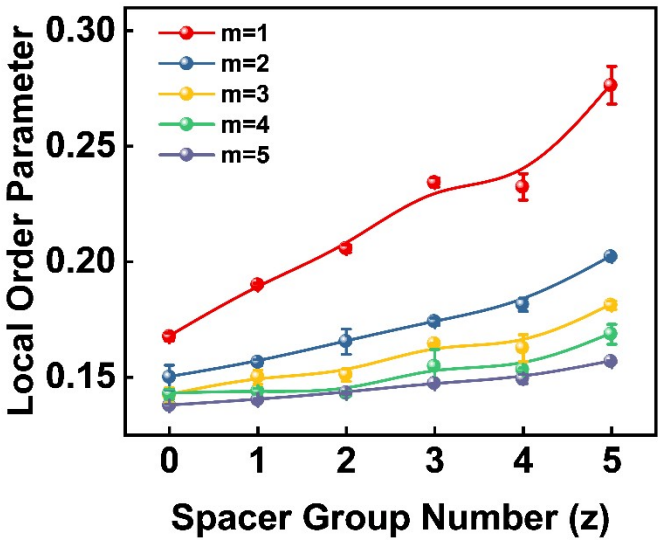

Fig. S5 Local order parameter of the rigid chains within the aggregates formed by A_{15}-g-(C_4/A-mR_3) with different spacer numbers *z* and rigid chain branches *m*.

References

1 P. J. Hoogerbrugge and J. M. V. A. Koelman, *Europhys. Lett.*, 1992, **19**, 155.

2 P. Español and P. Warren, *Europhys. Lett.*, 1995, **30**, 191.

3 R. D. Groot and P. B. Warren, *J. Chem. Phys.*, 1997, **107**, 4423-4435.

4 Y. Lv, L. Wang, F. Wu, S. Gong, J. Wei and S. Lin, *Phys. Chem. Chem. Phys.*, 2019, **21**, 7645-7653.

5 S. H. Chou, H. K. Tsao and Y. J. Sheng, *J. Chem. Phys.*, 2011, **134**, 034904.